Citation: Andrade, J., Legoinha, P., Stroynowski, Z., Abrantes, F. , 2019. Morphology, biostratigraphy, and evolution of Pliocene-Pleistocene diatoms Proboscia barboi and Proboscia curvirostris. *Geologica Acta, 17.9, 1-17.*
DOI: 10.1344/GeologicaActa2019.17.9

geologica acta

Morphology, biostratigraphy, and evolution of Pliocene-Pleistocene diatoms *Proboscia barboi* and *Proboscia curvirostris*

J. Andrade[1] P. Legoinha[2] Z. Stroynowski[3,4] F. Abrantes[3,4]

[1]Departamento de Ciências da Terra, Faculdade de Ciências e Tecnologia
Universidade Nova de Lisboa, 2829-516 Caparica, Portugal
Andrade E-mail: jpf.andrade@campus.fct.unl.pt

[2]Geobiotec, Faculdade de Ciências e Tecnologia
Universidade Nova de Lisboa, 2829-516 Caparica, Portugal
Legoinha E-mail: pal@fct.unl.pt

[3]Marine Geology Div, IPMA (Instituto Português do Mar e da Atmosfera)
Rua Alfredo Magalhães Ramalho 6, 1495-006 Algés, Portugal
Stroynowski E-mail: zuzia.stroynowski@ipma.pt
Abrantes E-mail: fatima.abrantes@ipma.pt

[4]CCMAR (Centro de Ciências do Mar do Algarve)
Universidade do Algarve, 8005-139, Faro, Portugal

ABSTRACT

Proboscia barboi and *Proboscia curvirostris* are two important diatom biostratigraphic markers from the high latitudes of the North Pacific and North Atlantic Oceans, dating back to the Pliocene-Pleistocene time. This study analyzes the biostratigraphic events and describes the morphology of *P. barboi* and *P. curvirostris*, particularly the morphologic variations of the latter species, based on observations of samples of Core U1340A from the IODP Expedition 323 in the Bering Sea. In Site U1340, the First Occurrence of *P. curvirostris* is observed at 1.52Ma and its First Common Occurrence at 1.39Ma, where morphologic variations were found abundantly. The Last Occurrence of *P. curvirostris* was found at 0.33Ma, while *P. barboi*'s Last Occurrence is found at 0.67Ma. Based on the morphological similarity and known biostratigraphic distribution, previous authors have assumed that *P. curvirostris* descends from *P. barboi,* although this hypothesis is still in debate. At 1.39Ma *P. curvirostris* shows an increased size and thickness, which is typical of *P. barboi*, and some specimens display an incipient structure characteristic of *P. curvirostris* - the secondary spine. This morphology is intermediate between the two species and suggests an evolutionary transition from *P. barboi* to *P. curvirostris*. However, *P. curvirostris* already existed since 1.9Ma in the subarctic indicating that its speciation happened much earlier than 1.39Ma. Furthermore, since *P. barboi* co-occurs with *P. curvirostris* in the North Pacific, this evolutionary process was cladogenetic. Besides being evidence for a phylogenetic relationship, the abundant occurrence of intermediate forms at 1.39Ma may constitute a bioevent for a short time interval in the Bering Sea.

KEYWORDS | **Probosciaceae. Proboscis. Longitudinal ridges. Site U1340. Quaternary.**

INTRODUCTION

Diatoms are unicellular photosynthetic algae formed by a silica shell named frustule and are considered the dominant marine primary producers, playing an important role in marine silica and carbon cycles (Mann, 1999; Tréguer and De la Rocha, 2013). Diatoms are an abundant and diverse phytoplankton group in the North Pacific Ocean where they are used to establish the age of deep sea sediments. Based on biostratigraphic events such as the First Ourrence (FO) or Last Occurrence (LO) of a taxon (referred to as datums), it is possible to construct high-resolution diatom biozonations that can be widely used for the detailed sub-division, dating and correlation of Neogene and Quaternary sediments (Akiba, 1986; Yanagisawa and Akiba, 1998). Extinctions and appearances of species are correlated to magnetochronology to obtain absolute age estimates of the diatom zones (Barron and Gladenkov, 1995). Like other microfossil groups, diatoms have also been successfully used to reconstruct past environments, providing information on climatic trends and ecological parameters of a given geographic area (*e.g.* Sancetta and Silvestri, 1986; Stroynowski *et al.*, 2017).

Proboscia is a marine genus of Probosciaceae Jordan et Ligowski with a wide geographical distribution that ranges in age from the Cretaceous Period to the present. Fossil species are commonly found in high latitudes of the Northern and Southern Hemisphere, in Subarctic and Antarctic waters, whilst extant *Proboscia* spp. Sundström have a worldwide ocean distribution (Jordan *et al.*, 1991; Jordan and Priddle, 1991; Takahashi *et al.*, 1994). *Proboscia barboi* is an extinct species, found in the mid- to high-latitudes of the North Pacific and North Atlantic Oceans but also in Southern high latitudes, as reported in Jordan and Priddle (1991). It is also a common biostratigraphic marker due to its robust and dissolution-resistant valve and wide geographic distribution. The species extends back to the Middle Miocene (Akiba and Yanagisawa, 1986) and its LO ranges from 0.3Ma (Yanagisawa and Akiba, 1998) to around 2Ma in the North Pacific (bottom of *Actinocyclus oculatus* zone; Koizumi, 1973). This variability can be explained either by diachrony (*i.e.* asynchronous extinctions), poor dating techniques, species misidentification or contrasting identification criteria. In the Atlantic Ocean *P. barboi* disappeared at 3.3Ma, 3Myrs earlier than its extinction in the Pacific Ocean (Koç and Scherer, 1996).

P. curvirostris is found in mid- to high-latitudes of the North Pacific and North Atlantic Oceans and stands out as an important Pleistocene biostratigraphic marker due to its short chronostratigraphic span and dissolution resistance. The FO of *P. curvirostris* is observed at 1.37-1.42Ma in the Bowers Ridge, IODP U1341 (Onodera *et al.*, 2016), 1.7Ma in the Bering Slope, IODP Site U1343 (Teraishi *et al.*, 2016), 1.58Ma in the Western Subarctic (ODP Sites 881 to 884 and 887; Barron and Gladenkov, 1995), 1.6Ma in the North-West Pacific around Japan (Yanagisawa and Akiba, 1998) and even at 1.9Ma in the subarctic Pacific, Sites 192 and 183 (Koizumi, 1973; Koizumi, 2010). The LO of *P. curvirostris* defines the youngest datum of Pliocene-to-present sequences in the North Pacific and is generally established at 0.3Ma (Koizumi, 2010; Expedition 323 Scientists, 2001; Yanagisawa and Akiba, 1998), although the LO varies between 0.26 and 0.35Ma in the North Pacific, depending on location (Barron and Gladenkov, 1995; Koizumi and Tanimura, 1985; Onodera *et al.*, 2016; Teraishi *et al.*, 2016). In the northern North Atlantic, *P. curvirostris* disappeared at 0.31Ma, since this region is more sensitive to climatic forcing (Irminger Basin, ODP 919). In contrast, in the mid latitudes (~40ºN) it lasted until 0.26Ma (Koç *et al.*, 2001). The age correspondence between the North Atlantic and North Pacific suggests that this event was relatively synchronous in both oceans (Koç *et al.*, 2001).

The preserved fossil remains of *P. barboi* and *P. curvirostris* correspond to the broken tubular structure (the proboscis) projecting from the valves. These species were previously accommodated within genus *Rhizosolenia* Brightwell but were later transferred to the genus *Proboscia* Sundström along with several other species, based on the strong resemblance of the valve fragments to a proboscis and the lack of external process, such as that found in *Rhizosolenia*. Two other diagnostic characters define this genus: the spinulae and the longitudinal slit located at the distal end of the proboscis. The latter feature is assumed to be associated with the rimoportula (labiate process) - an opening through the valve wall that extends internally and is surrounded by two lips (Hasle *et al.*, 1996; Jordan *et al.*, 1991; Jordan and Priddle, 1991; Takahashi *et al.*, 1994).

Morphologic variations of diatom frustules, such as those found in resting spores and/or resting stages, may arise in response to unfavorable changes in the environmental conditions. The morphology of the resting spore may differ so considerably from that of the vegetative valve that they may be assigned to different species thereby giving rise to taxonomic confusion (Hargraves, 1986). Resting spores and resting stages can typically account for most of the fossil assemblage, due to their greater resistance to dissolution (Barron, 1985; Tsukazaki *et al.*, 2013). Furthermore, there are also morphologic variations in which some forms display a mixture of characteristics of two closely related species, making them potential intermediate forms and suggesting an evolutionary relationship between species. A well-studied example is *Neodenticula* sp. A of Akiba et Yanagisawa (1986) an intermediate form between *Neodenticula koizumii* (extinct) and *Neodenticula seminae*.

In this study, the morphology of *P. barboi* and *P. curvirostris* is described and illustrated with high resolution Scanning Electron Microscopy (SEM) and Light Microscopy (LM) images, and their biostratigraphy for Core U1340A (IODP Expedition 323) presented and discussed. Furthermore, the evolution of *P. curvirostris* is discussed in light of the described morphological variations.

GEOGRAPHICAL AND GEOLOGICAL SETTING

The Bering Sea is characterized by its extensive eastern continental shelf, which covers roughly half of its area from northwest to southeast, creating a vast neritic area (<200m, Fig. 1) that is seasonally covered by ice. The central and southern area consists of the Aleutian Basin (3500m deep) with two main structural highs: the Bowers Ridge, which extends from the Aleutian Island arc into the Aleutian Basin; and the Shirshov Ridge extending from Kamchatka, Siberia. Three main rivers flow into the Bering Sea: the Kuskokwim and Yukon rivers drain Central Alaska, and the Anadyr River drains Eastern Siberia. Of the three rivers, the Yukon River supplies the largest discharge into the Bering Sea, with a mean annual flow of $5x10^3$ m^3s^{-1}, roughly the same as the annual flow of the Mississippi (Takahashi, 2005).

The surface water circulation of the Bering Sea Basin follows a large-scale cyclonic gyre. The main source of water input to the Bering Sea comes from the Alaskan Stream flowing westward along the Aleutian Islands (Stabeno et al., 1999). Water exchange in the Bering Sea has changed in the past as a consequence of glaciations which altered the eustatic levels and thereby influenced the differential amount of water flow through the Aleutian passes. For example, during glacials, due to the closure or restriction of eastern passages (*e.g.* Amchitka Strait), the alaskan stream entered the Bering Sea through passages further west (*e.g.* Buldir Pass), allowing sea ice to extend from the Umnak Plateau to the crest of the Bowers Ridge (Katsuki and Takahashi, 2005). One of the most drastic changes in water exchange in the Bering Sea was the closure of the Bering Strait during the last glacial maximum, which became aerially exposed due to the decrease in sea level (Chappell *et al.*, 1996).

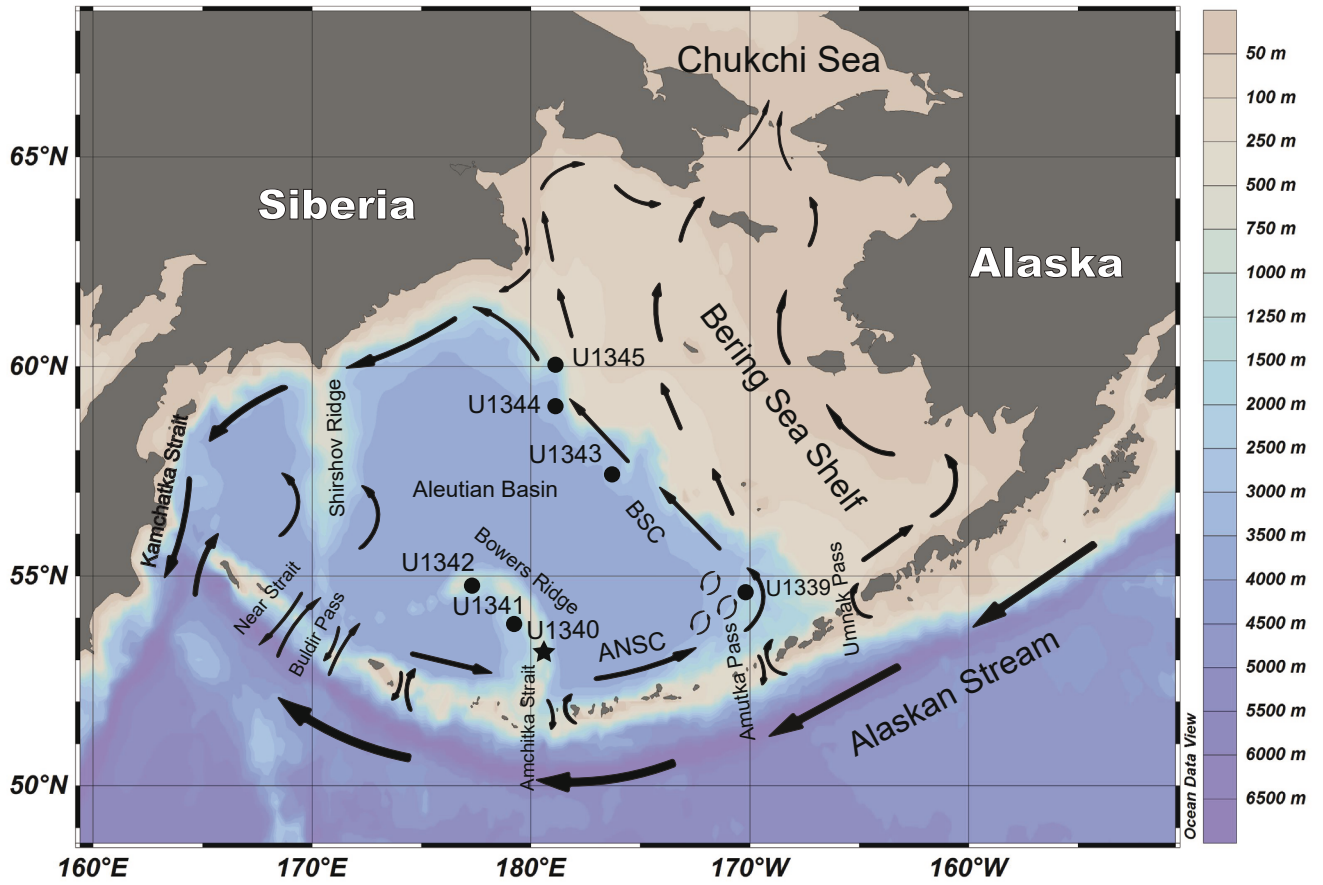

FIGURE 1. Map of the Bering Sea with the location of Site U1340 (black star) and other sites (black circles) of the IODP Expedition 323. Surface water currents are indicated by arrows. Water depth scale is provided on the right. Map generated by Ocean Data View 4.0. ANSC: Aleutian North Slope Current.

Bering Sea has been a region of interest to the study of the stratigraphy and paleoceanography of the Neogene and Quaternary periods due to its high responsiveness to global climate changes caused by glacial-interglacial cycles. The Integrated Ocean Drilling Program (IODP) Expedition 323 executed a series of deep ocean drillings in the Bering Sea, in three different areas: the Umnak Plateau, the Bowers Ridge and the Bering Slope region, covering the past 5Ma, depending on the drilling sites (Takahashi *et al.*, 2011). Site U1339, in the Umnak Plateau, reached 0.74Ma. In the Bowers Ridge, Cores U1340A and U1341B retrieved sediments going back to 5Ma and 4.3Ma respectively. The latter age was later revised to 5Ma, by an onshore study from the shipboard data (Expedition 323 Scientists, 2010). In the Bering Slope region, Hole U1343E reached 2.4Ma, whereas Hole U1344A reached 1.9Ma. The cores retrieved from the Bowers Ridge Sites U1340 and U1341 display high mean sedimentation rates, approximately 12cm/ky, while in the Bering Slope sedimentation rates are even higher (21–58cm/ky in Hole U1343E and 29–50cm/ky in Hole U1344A), mainly due to the deposition of silt and clay transported from the Yukon river and other rivers (Takahashi *et al.*, 2011).

Based on the lithostratigraphic patterns and as suggested by the results of Expedition 323, the sedimentation history in the Bering Sea can be divided into three main phases established around: 5-2.7Ma (Unit III), 2.7-1.7Ma (Unit II) and 1.74-recent (Unit I). In Site U1340, where the samples of this study were retrieved, the Unit III/II boundary is defined by a change from sponge-spicule bearing sand (Subunit IIIA) to diatom ooze sediments (Unit II). The Unit II/I boundary is marked by a passage to sediments alternating between diatom ooze and diatom silts (Expedition 323 Scientists, 2011).

Since the 1970s, several other drilling projects were made in the North Pacific which enabled the construction of a diatom biozonation for the North Pacific (Barron and Gladenkov, 1995; Koizumi, 1973; Koizumi and Tanimura, 1985; Koizumi, 2010; Onodera *et al.*, 2016; Schrader, 1973; Teraishi *et al.*, 2016; Yanagisawa and Akiba, 1998). The biostratigraphy in Hole U1340A follows these biozonations and was constructed to reach the early Pliocene (Expedition 323 Scientists, 2011).

MATERIALS AND METHODS

IODP Expedition 323 carried out extensive drilling in the Bering Sea (Fig. 1). The samples used in this study were collected from Core U1340A (Expedition 323 Scientists, 2011), which was recovered from the southeastern flank of the Bowers Ridge at 1295m water depth and reached 604.5mbsf.

During routine taxonomic counting of upper Pleistocene samples of Core U1340A, morphologic variations of *P. barboi* and *P. curvirostris* were occasionally observed throughout the sample set, but Sample U1340A-24H-5 (203.54mbsf; 1.39Ma) was particularly rich in specimens showing such morphologic variations. The specimens from this sample were studied and illustrated through SEM imaging, along with a few other samples containing *P. curvirostris* (U1340A-24H-3, 200.54mbsf; U1340A-18H-3, 160.39mbsf) and *P. barboi* (U1340A-26H-3, 219.55mbsf; U1340A-25H-5, 213.04mbsf). These samples are listed in Table 1 and were selected based on the abundance and preservation quality of the valve fragments of the target species. However, besides the samples selected for SEM imaging, 40 samples of Core U1340A (from 4H-CC, 32.56mbsf to 28H-3, 238.55mbsf) were

TABLE 1. List of studied samples of Core U1340A. Depth and age follow Stroynowski *et al.* (2015)

Core U1340A sample ID	Section Mid-depth (cm)	Site Depth (mbsf)	Age (Ma; ±0.1)
5H-CC	0.5	42.13	0.3271
11H-CC	0.5	99.17	0.6688
18H-3	150	160.39	1.1022
23H-3	136	191.04	1.3087
24H-3	136	200.54	1.3727
24H-5	136	203.54	1.3929
25H-3	136	210.04	1.4367
25H-5	136	213.04	1.4569
26H-3	136	219.55	1.5008
26H-5	136	222.55	1.5210

thoroughly observed at the LM. All the observed samples belong to Unit I (U1340A-1H-1 through 32H-2) of Core U1340A. The ages corresponding to each sample of Core U1340A follow Stroynowski *et al.* (2015), were rounded to hundredths and have a ±0.1Ma relative error margin. The samples and LM slides are deposited in IPMA (Instituto Português do Mar e da Atmosfera, Algés, Portugal) under the sequence: Exp323-U1340A-XH-Y, where XH identifies the core section and Y the depth (cm) in core sections.

The laboratory procedure for sample treatment follows the methodology of Abrantes *et al.* (2005). A modification to the procedure was made as regards the amount of sample used for SEM observations. In this case, a reduced amount of 0.3g of wet sediment was processed. The washing technique of mixing and 8 hour settling process was used until samples reached pH ~7. Afterwards, sieving was performed to concentrate the target species and eliminate the valves and debris smaller than 15μm.

TABLE 2. Measurements of specimens from Sample U1340A-24H-5 (203.54mbsf), except Figure 8F (U1340A-24H-3; 200.54mbsf) and Figure 8L (U1340A-24-CC; 203.54 – 210.04mbsf). The curvature of specimens in Figures 6A; 7D, J was not measured due to the incomplete proximal part or unsuited position of the valve

Figure	width (µm)	Curvature (°)
6A	11.6	-
6B	11.3	95
6C	11.3	100
6D	12.3	100
6E	12.9	97
6F	11.9	107
6G	12.1	120
6H	11.5	108
6I	11.1	96
6J	11.9	108
7A	8.9	87
7D	9.4	-
7F	9.2	98
7G	9.3	98
7J	10	-
7K	10.5	115
8D	9.4	95
8E	7.5	92
8F	8.3	86
8G	8.8	95
8H	9.3	100
8I	8	112
8J	8.3	87
8K	9.6	87
8L	9.4	106
Mean	10.2	99.5

Besides the secondary spine, which is the diagnostic feature that distinguishes *P. curvirostris* from *P. barboi*, the width and the curvature of the proboscis fragments were used as the main taxonomic criteria to distinguish both species (Table 2). The width (μm) was measured at the region between the maximum curvature and the tip of the proboscis, closer to the former, as the proboscis in some specimens appears to become narrower towards the apex. The curvature (°) of the proboscis was measured on the ventral side (Fig. 2).

Diatom terminology follows mostly Jordan and Priddle (1991) but a few terms were taken from Akiba and Yanagisawa (1986; striae, puncta, dorsal and ventral poles), Takahashi *et al.* (1994; longitudinal ridges, transversal ribs) and some are used here originally when appropriate (lobe, incipient, normal and parallel orientations).

RESULTS

Valve morphology

The valve fragments of *P. barboi* and *P. curvirostris* preserved in the sediments correspond to the proboscis: a hollow and curved tube bearing two large spines and several smaller spines, *i.e.* spinulae, at the distal end (Fig. 3). This region is elliptical in outline, defining a dorsal pole and a ventral pole. The longitudinal slit is also located at the distal end and is a diagnostic feature of *Proboscia*, thought to be the external part of the rimoportula, an opening on the valve wall that connects with an internal flattened tube (Jordan *et al.*, 1991; Jordan and Priddle, 1991). Striae run along the length of the proboscis and some shorter striae are only present at the distal end.

The main differences between the two species reside in the fact that *P. curvirostris* is smaller, thinner, considerably more curved and, most importantly, bears a secondary spine which is diagnostic (Akiba and Yanagisawa, 1986; Jordan and Priddle, 1991). The terms dorsal and ventral are commonly used to refer to the convex and concave sides of the proboscis, respectively (Fig. 3).

Proboscia barboi

P. barboi consists of a long and curved hollow tube generally well above 90° of curvature and 10 to 12μm width (Fig. 4A-H) with some rare exceptions such as the thinner specimen illustrated in Figure 4E.

The distal end is an important region of the proboscis since it is there where most features concentrate, such as the spines and the longitudinal slit (Fig. 4B, D, F, H). The spine at the dorsal pole is typically oriented at 90° to the longitudinal

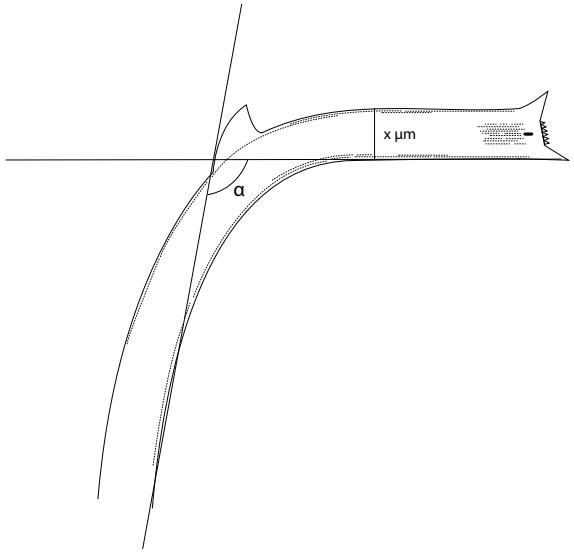

FIGURE 2. Measurement of the proboscis width (x µm) and curvature (α °).

axis of the proboscis, while the spine at the ventral pole extends distally (*i.e.* normal orientation; Fig. 4C, G-H), although occasionally both spines point distally (*i.e.* parallel orientation; Fig. 4E-F). The size of the spines is variable.

Small spines, named spinulae, are located at the tip of the proboscis between the two large spines and have variable dimensions. They are positioned either in regularly spaced intervals with uniform dimensions (Fig. 4D), or in a more disorganized, dense fashion with different sizes (Fig. 4F-H).

Located immediately below the tip of the distal end, is the longitudinal slit (Fig. 4B, D), a characteristic feature of *Proboscia*, which is thought to be the external part of the rimoportula (Jordan *et al.*, 1991; Jordan and Priddle, 1991). The longitudinal slit is only present on one side of the proboscis.

The proboscis is ornamented by uniseriate striae composed of two groups of longitudinal rows. One consists of long and parallel rows lining both dorsal and ventral sides, from the distal end to the proximal regions (Fig. 4B, D). The rows have variable lengths and start at different points of the proboscis. The other group of striae is formed by short and parallel rows restricted to the distal end, on both lateral sides (Fig. 4B, D, F, H). These rows are frequently interrupted, and the density of puncta is variable. The short rows on the distal end can sometimes be observed on the LM. However, the long longitudinal rows require SEM imaging to be visible.

Proboscia curvirostris

P. curvirostris is noticeably thinner and more curved than *P. barboi*, being usually below 10μm width and roughly around 90º (Fig. 5A-J). It bears a secondary dorsal spine, which is diagnostic and distinguishes it from *P. barboi* (Fig. 5A-B, D-E, H-I). Most of the remaining morphologic features are shared by both species and their description is equally applicable with slight differences here described.

The spines at the distal end have a normal orientation like *P. barboi* (Fig. 5F, J). However, the parallel orientation (both spines oriented distally) occasionally found in *P. barboi* is not present in *P. curvirostris*. The secondary spine is located at the point of strongest curvature on the dorsal side of the proboscis. This spine varies frequently

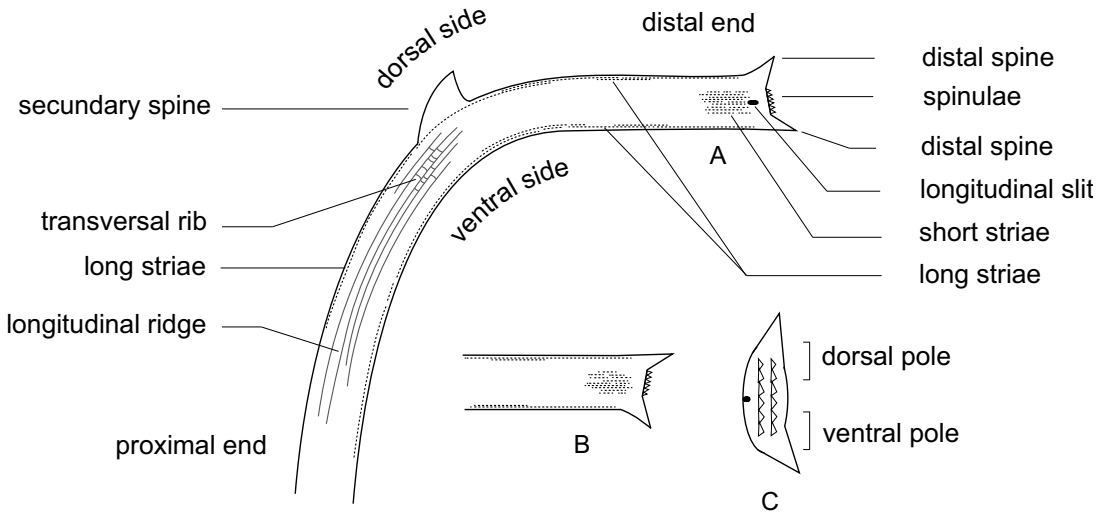

FIGURE 3. Terminology of the proboscis of *P. curvirostris*, equally applicable to *P. barboi*. A) Side view showing longitudinal slit. B) Side view without longitudinal slit. C) Frontal view of the distal end of A.

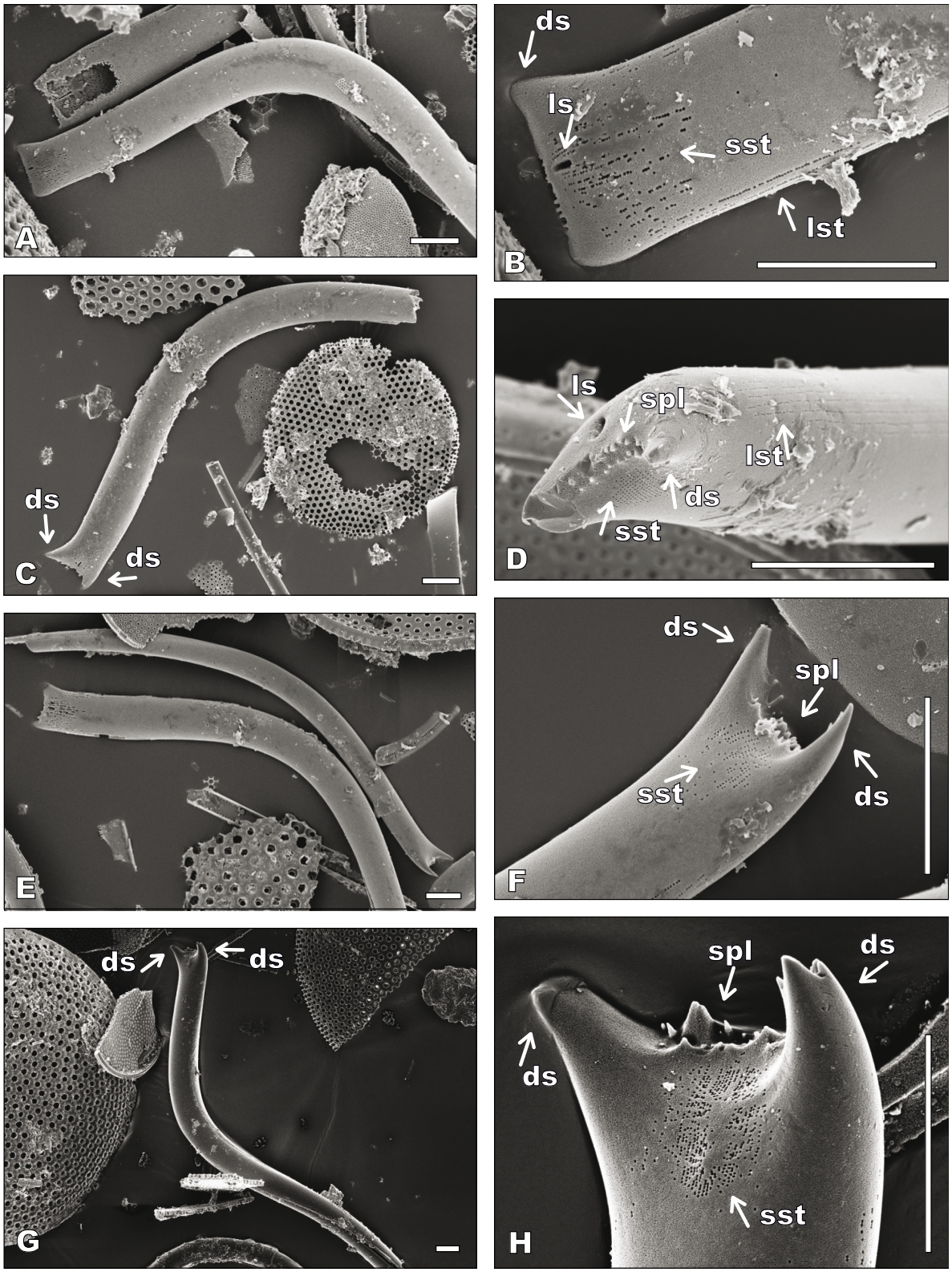

FIGURE 4. *Proboscia barboi*. SEM images. Scale bars= 10µm. A) Well preserved specimen. B) Close-up view of A showing the distal end of the specimen with the longitudinal slit (ls), long longitudinal striae (lst), short longitudinal striae (sst) and distal spines (ds) C) Specimen with normal orientation of the distal spines (ds). D) Distal end of specimen in C showing the spinulae (spl) lining the tip, longitudinal slit (ls), long striae (lst) and short striae (sst). E) Two specimens with contrasting widths. F) Detail of the distal end of the slender specimen in E showing parallel orientation of distal spines (ds). G) Specimen showing irregular spinulae (spl) between spines (ds). H) Close-up view of G. All specimens are from Sample U1340A-26H-3, 136cm.

according to height and length parameters, but its tip always points towards the distal end. Sporadically, the secondary spine displays two or more tips or lobes (Fig. 5I). This variation is particularly abundant in Sample U1340A-24H-5 (203.54mbsf) and can also be observed between Samples U1340A-26H-5 and 24H-3 (222.55 to 200.54mbsf), where *P. curvirostris* is scarce.

The longitudinal slit, long rows of striae, short rows restricted to the distal end and spinulae, can be observed in specimens illustrated in Figure 5C, F-G, J. Specimens in Figure 5F, J show different arrangements of spinulae, the former being disorganized and the latter showing a remarkable regular arrangement and size. Torsion of the proboscis is occasionally present to different extents and is more frequent than in *P. barboi*. In Figure 5D, a slight torsion of the proximal region of the proboscis can be observed.

In specimens from Sample U1340A-18H-3 conspicuous longitudinal ridges were observed along the external surface of the proximal part of the proboscis until the point of strongest curvature (Figs. 3; 5A-B, D-E, H-I). The longitudinal ridges accompany the curvature of the proboscis, vary in length and may occasionally branch into two or converge. In some specimens, adjacent ridges are connected by a series of transversal ribs (Fig. 5E, I). Shorter or less marked ridges, some with a faint appearance were also found in *P. curvirostris* specimens of Samples U1340A-24H-5 and 24H-3. Other ridge-like structures have been found before in both fossil and extant *Proboscia* spp. (Jordan and Saito, 1999; Jordan and Ito, 2002; Jordan and Ligowski, 2004). Particularly, the described longitudinal ridges are strikingly similar to those found in *Proboscia subarctica* TAKAHASHI, JORDAN et PRIDDLE, including the transversal ribs, although in this species the ridges are more linear, regular, and cover most of the length of the proboscis (Takahashi *et al.*, 1994). No ridges were observed in *P. barboi*, which displayed a smooth surface.

Intermediate forms

In Sample U1340A-24H-5 (203.54mbsf; 1.39Ma) *P. curvirostris* displays a size notably larger than what is observed in other samples of the core. Besides the larger size, many specimens were thicker, frequently above 11μm width, thus comparable to *P. barboi* (Fig. 6; Table 2). This unusual proboscis width was not observed in any other sample of Core U1340A. Besides the considerably higher proboscis proportions, several variations of the secondary spine were observed in these specimens. Some secondary spines were shorter and longer (Figs. 7F-H; 8H-K) or too small and not oriented (incipient) as in Figures 6F-G, J; 7K-L. Another interesting variation is the secondary spine with two or more tips or lobes (multi-lobed), sometimes isolated enough to form more than one separate spine (Figs. 6G; 7A-B; 8D-E, G). These types of secondary spine (long, incipient, and multi-lobed) are here considered extreme variations and are rare in specimens from Core U1340A. They are also found in specimens from Samples U1340A-26H-5, 26H-3, 25H-3, 24H-CC and 24H-3, although *P. curvirostris* is very scarce and its size is average (Fig. 8F, L). It is noteworthy that secondary spines with two lobes were already mentioned by Akiba and Yanagisawa (1986) and Loseva (1990) who called them "bi-triangular" and "two-apex" spines respectively.

The curvature of the proboscis is generally not very different from that of typical *P. curvirostris* proboscis (Table 2). Some specimens have a curvature degree above average (*e.g.* Figs. 6G-H, J; 7K), but this variation can also be observed in typical *P. curvirostris*. The distal spines are normally oriented. The spinulae, longitudinal slit, and long and short rows of striae, can be observed in the specimens in Figure 7C, E, L.

Although longitudinal ridges are uncommon in *P. curvirostris* specimens from Sample U1340A-24H-5, marked ridges can be observed in the specimen in Figure 7D while Figure 7G, I, shows a specimen whose longitudinal ridges are noticeably fainter and further apart from each other.

Sratigraphic range

Proboscia barboi occurs from the base of Core U1340A (Stroynowski *et al.*, 2015) to Sample U1340A-24H-5 (203.54mbsf) and is absent in the overlying samples, except in Sample U1340A-23H-3, where it is scarcely represented, and in Sample U1340A-11H-CC (99.17mbsf; 0.67Ma) where it is abundant. Although *P. barboi* is absent in the levels above Sample U1340A-24H-5 for a period of 0.72Ma, its reappearance in Sample U1340A-11H-CC with abundant specimens marks its LO (Figs. 9; 10; Table 3).

Proboscia curvirostris appears in Sample U1340A-26H-5 (222.55mbsf; 1.52Ma) which marks its FO. In this sample, *P. curvirostris* is scarce and represented by specimens with secondary spine variations. Nonetheless, they displayed a secondary spine of some form or variation, thus they were considered *P. curvirostris*. These specimens occur scarcely from Sample U1340A-26H-5 to 24H-3 (222.55-200.54mbsf; 1.52-1.37Ma). Sample U1340A-24H-5 (203.54mbsf; 1.39Ma) is important as *P. curvirostris* occurs abundantly, thus marking its First Common Occurrence (FCO). In this sample, it displays a significantly larger length and width and variations of the secondary spine. The LO of *P. curvirostris* was observed

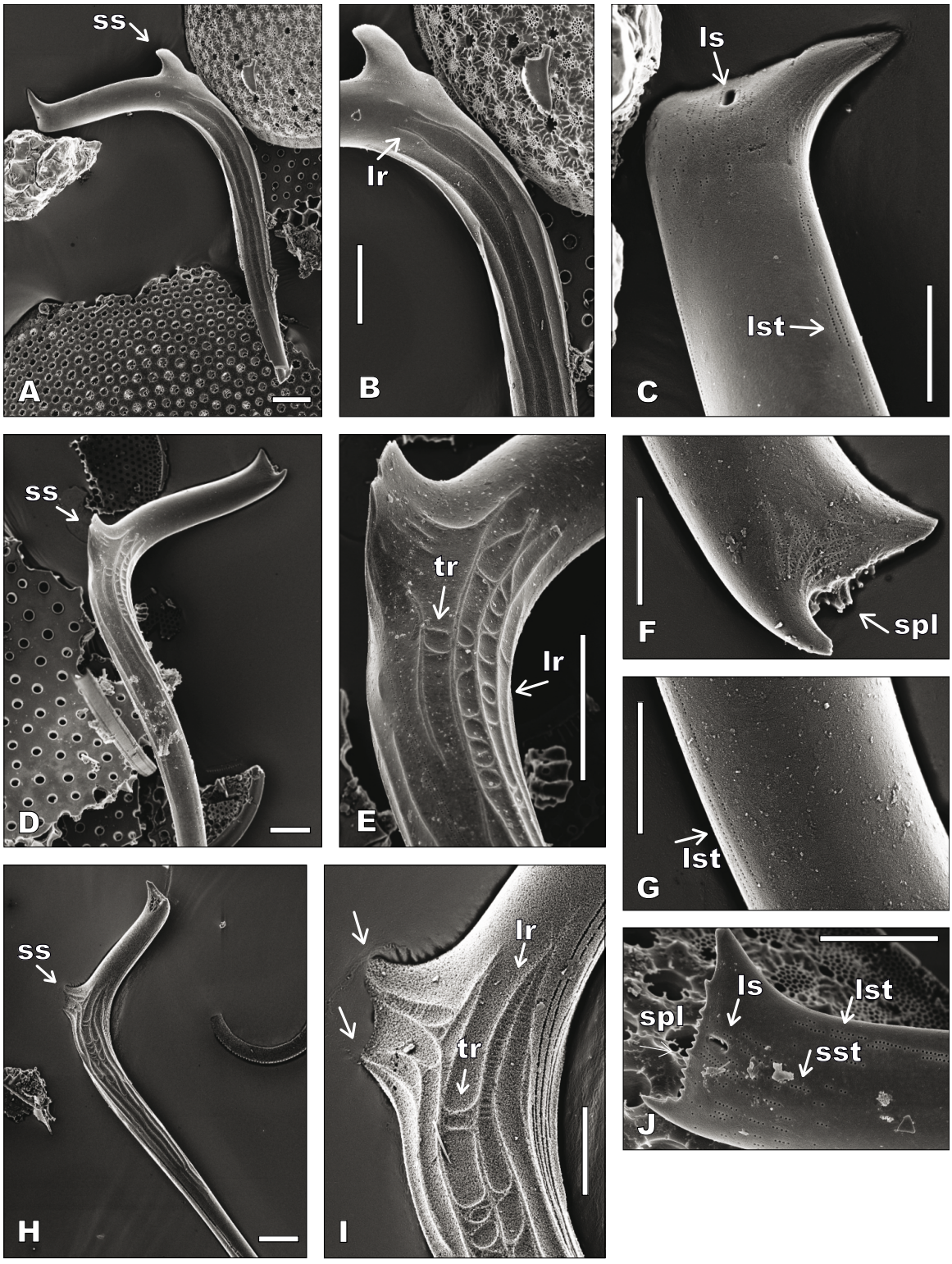

FIGURE 5. *Proboscia curvirostris*. SEM images. Scale bars= 10µm in A, B, D, E, G, and =5µm in C, F, H, I, J. A) Specimen displaying the secondary spine (ss). B) Close-up view of A, showing the longitudinal ridges (lr). C) Distal end of specimen in A showing the longitudinal slit (ls) and long striae (lst). D) Specimen displaying the secondary spine (ss). E) Close-up view of D, showing the longitudinal ridges (lr) and transversal ribs (tr). F) Distal end of specimen in D showing the spinulae (spl). G) View of a distal region of specimen in D showing long striae (lst). H) Specimen with a two-lobed secondary spine (ss). I) Close-up view of H showing the longitudinal ridges (lr), transversal ribs (tr) and the secondary spine with two lobes (arrowed). J) Distal end of specimen in H displaying regular spinulae (spl), longitudinal slit (ls), long striae (lst) and short striae (sst). All specimens are from Sample U1340A-18H-3, 150cm.

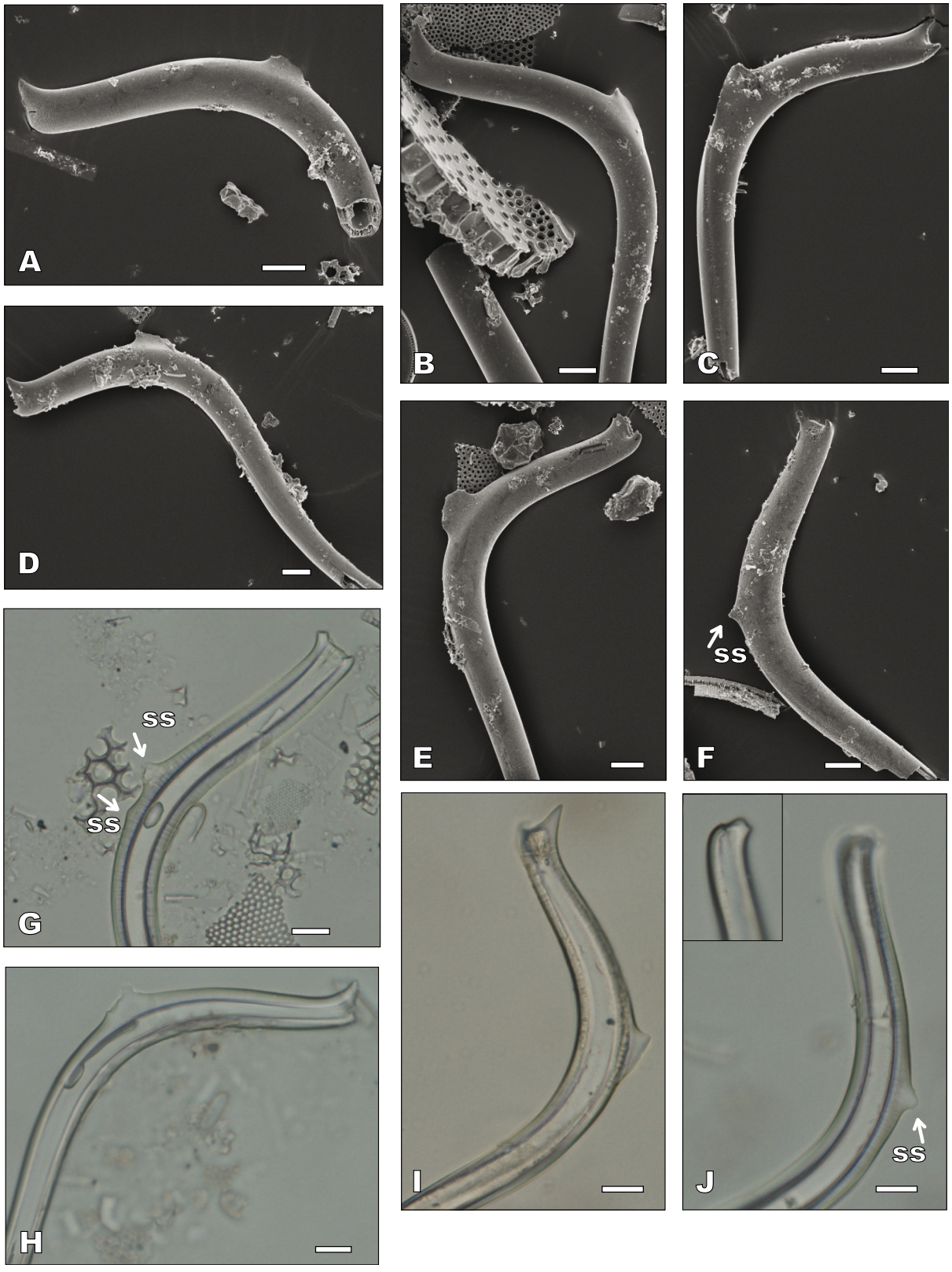

FIGURE 6. *Proboscia curvirostris* (intermediate forms). A-F are SEM images and G-J LM images. Scale bars= 10µm. A-E) Specimens with average or small secondary spines. F) Specimen with incipient secondary spine (ss). G) Specimen with two incipient secondary spines (ss). H-I) Specimens with average or small secondary spines. J) Specimen with incipient secondary spine (ss) and, inserted, close-up view of its distal end. All specimens are from Sample U1340A-24H5, 136cm.

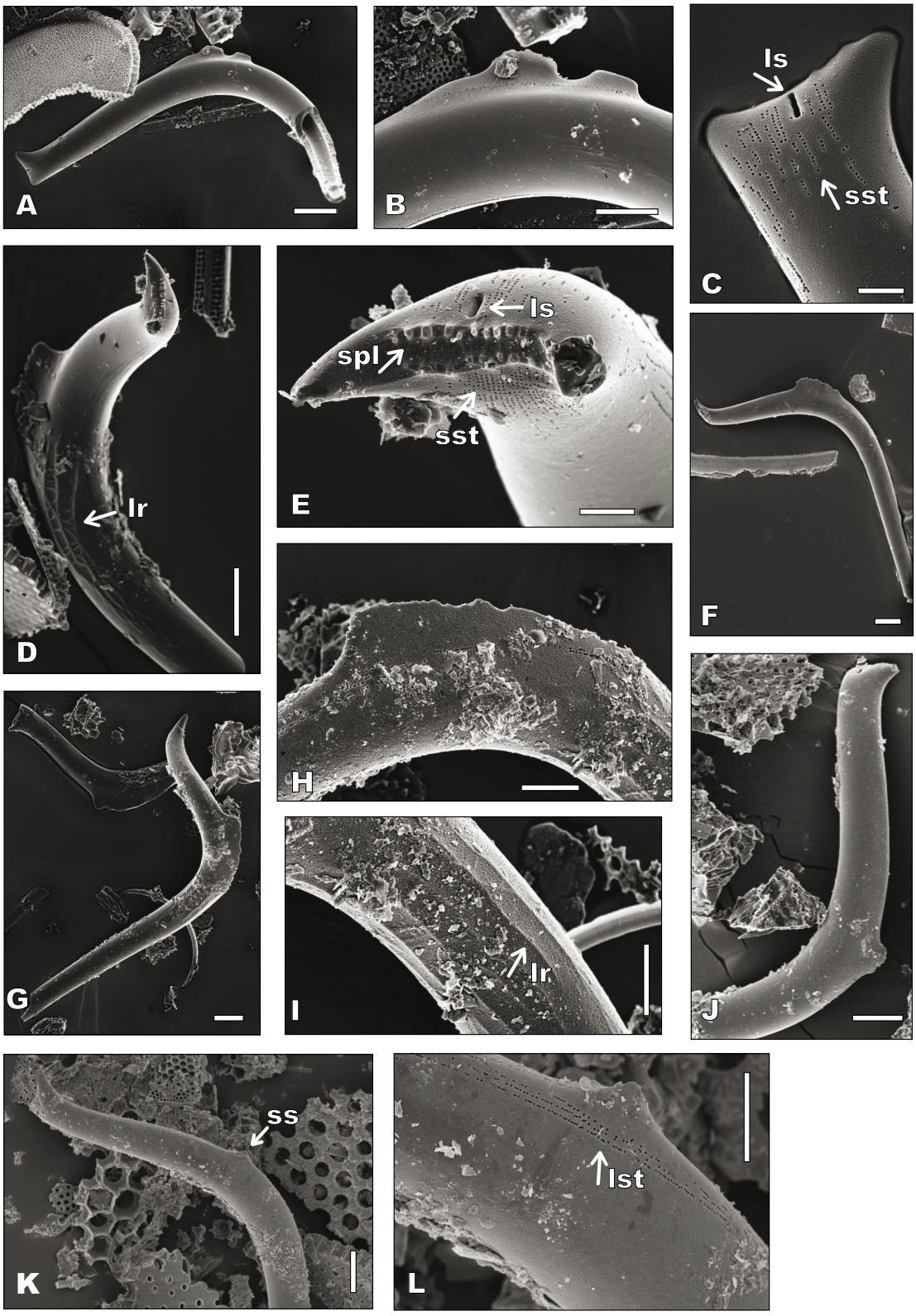

FIGURE 7. P*roboscia curvirostris* (intermediate forms). SEM images. Scale bars= 10µm in A, D, F, G, J, K. 5µm in B, H, I, L and 2µm in C, E. A) Specimen with two-lobed secondary spine. B) Close-up view of A. C) Close-up view of the distal end of the specimen in A showing the longitudinal slit (ls) and short striae (sst). D) Specimen with longitudinal ridges (lr). E) Close-up view of the distal end of specimen in D showing the longitudinal slit (ls), short striae (sst), and spinulae (spl). F-G) Specimens with a long secondary spine. H) Detail of secondary spine of specimen in G. I) Detail of faint longitudinal ridges (lr) of specimen in G. J) Specimen with a short secondary spine. K) Specimen with incipient secondary spine (ss). L) Close-up view of K showing the secondary spine and long striae (lst). All specimens are from Sample U1340A-24H5, 136cm.

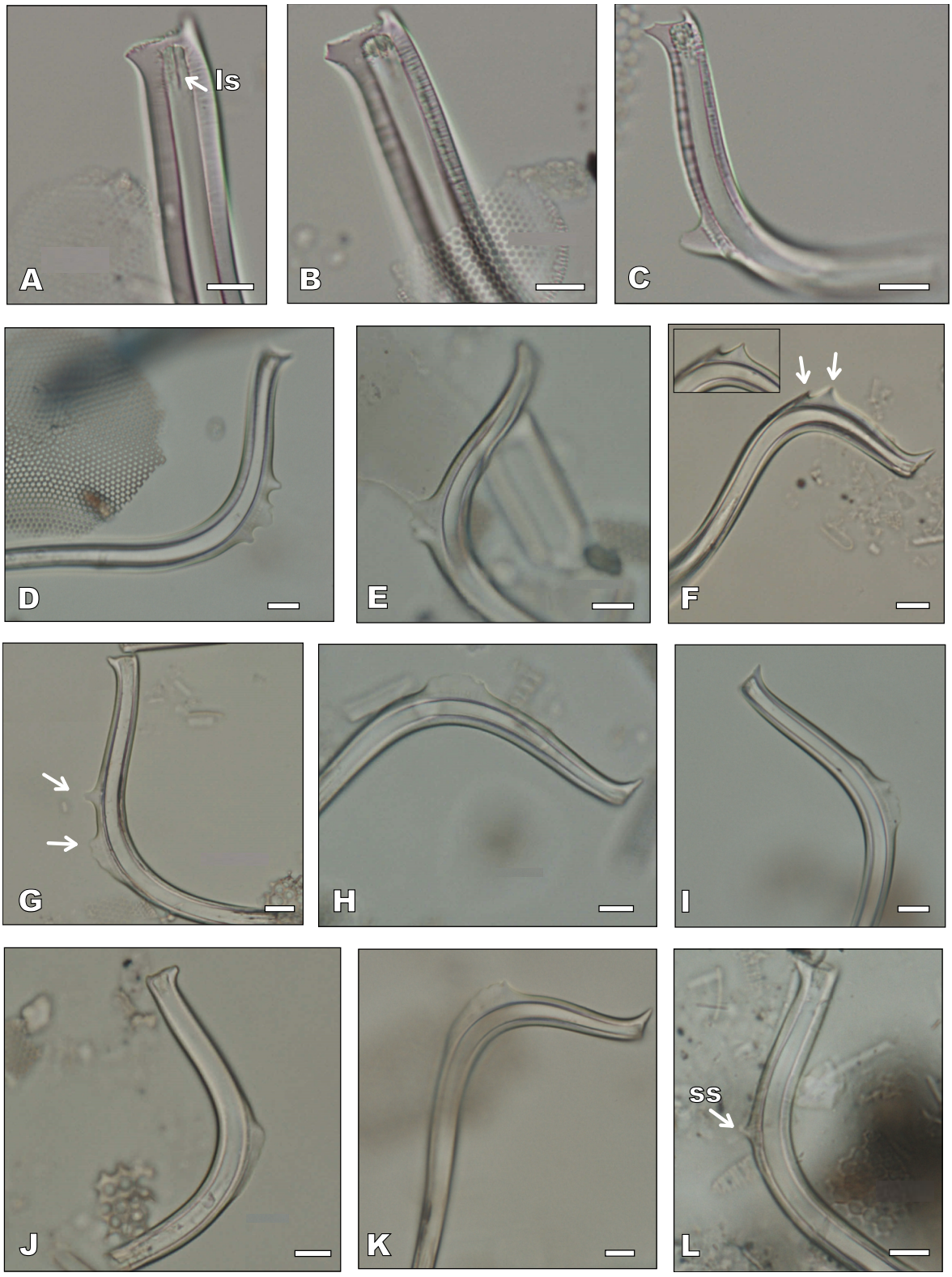

FIGURE 8. LM images of *Proboscia barboi*, *P. curvirostris* and intermediate forms. Scale bars= 10µm. A-B) distal end of *P. barboi* specimens; longitudinal slit (ls) is visible in A. C) *P. cuvirostris* with a typical secondary spine. D-E) Intermediate forms with a multi-lobed secondary spine. F) P. curvirostris with two secondary spines (arrows) and inserted, their close-up view. G) Intermediate form with two secondary spines (arrows). H-K) Intermediate forms with a long secondary spine; L) *P. curvirostris* with an incipient secondary spine (ss). All specimens are from Sample U1340A-24H5, 136cm), except specimens in A-B (Sample U1340A-26H-3, 136cm), in C (Sample U1340A-14H-3, 105.5cm), in F (Sample U1340A-24H-3, 136cm) and in L (Sample U1340A-24H-CC, 136cm).

in Sample U1340A-5H-CC (42.13mbsf, 0.33Ma; Figs. 9; 10; Table 3).

DISCUSSION

Intermediate forms and phylogeny of *P. barboi* and *P. curvirostris*

Much of the evidence for evolution is based on the observation of forms and/or structures intermediate between two taxa, which represent the transition to and rise of a new species or morphotype such as in the example of *Neodenticula* sp. A of Akiba et Yanagisawa (1986).

The phylogenetic affinities of *P. barboi* and *P. curvirostris* are under debate. Akiba and Yanagisawa (1986) stated that *P. barboi* evolved from *Proboscia praebarboi* JORDAN et PRIDDLE, which shows a straight and simple-ended proboscis, and that *Proboscia barboi* evolved into *P. curvirostris*, by developing a smaller and markedly curved proboscis bearing a secondary dorsal spine, thereby forming a continuous evolutionary lineage. However, Jordan and Priddle (1991) remarked that the occurrence of earlier taxa with curved proboscis that bear terminal large spines argues against this hypothesis. Furthermore, Hajós (1976) suggested that the Oligocene species *Rhizosolenia interposita* HAJÓS (now *Proboscia interposita* JORDAN et PRIDDLE) is an intermediate form between *Proboscia cretacea* JORDAN et PRIDDLE and *P. curvirostris*. An intermediate form between *P. barboi* and *P. curvirostris* was also reported by Jouse (1971). This form lacked the secondary spine and occurred from the late Pliocene to early Pleistocene, but, as far as could be ascertained, not much research has been carried out on this form.

P. curvirostris from Sample U1340A-24H-5 (1.39Ma; Figs. 6; 7; 8) shows a proboscis length and width comparable to *P. barboi*, sometimes surpassing 11μm width (Fig. 6). Furthermore, it frequently displays a secondary spine of unusual shape: incipient (Figs. 6F-G, J; 7K-L), long (Fig. 7F-H) or multi-lobed (Fig. 6G; 7A-B; 8D-E, G). Given that these specimens display features of *P. curvirostris* (the secondary spine) and *P. barboi* (length/width), they are regarded here as intermediate forms between both species. Particularly, specimens with an incipient secondary spine are the best example for this intermediate morphology and together with other intermediate forms point towards an evolutionary transition. The secondary spine variations seem to affect both intermediate forms and normal sized scarce *P. curvirostris* specimens during 1.52-1.37Ma.

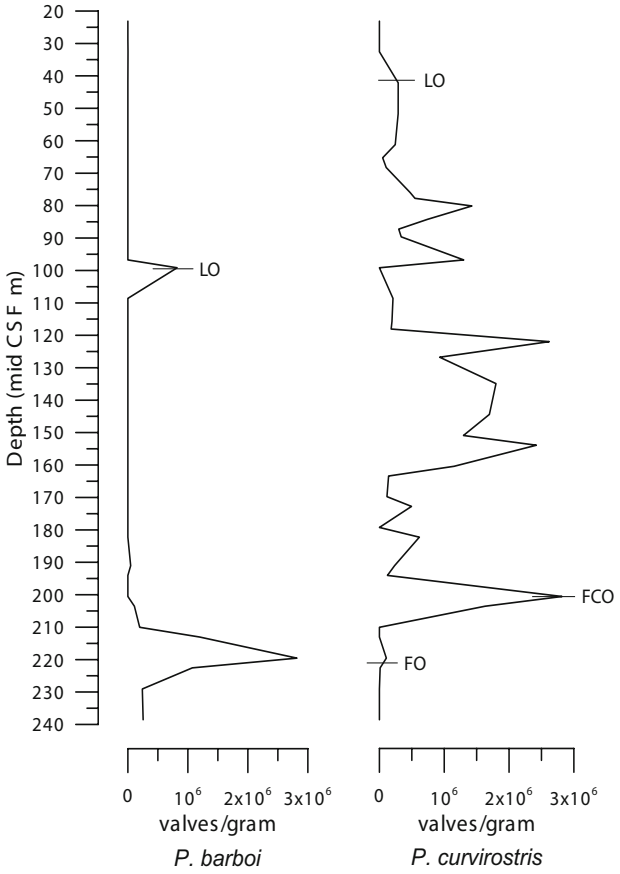

FIGURE 9. Plot of the productivity (valves/gram) of *P. barboi* and *P. curvirostris* in Core U1340A. FO: First Occurrence. FCO: First Common Occurrence. LO: Last Occurrence.

TABLE 3. Datums of *P. curvirotris* and *P. barboi* of Core U1340A with corresponding sample number, depth and age

	Datum	Sample	Depth (mbsf)	Age (Ma)
P. curvirostris	LO	U1340A-5H-CC	42.13	0.33-0.26
	FCO	U1340A-24H-5	203.54	1.44-1.39
	FO	U1340A-26H-5	222.55	1.52-1.56
P. barboi	LO	U1340A-11H-CC	99.17	0.67-0.65
	LCO	U1340A-25H-3	210.04	1.44-1.39

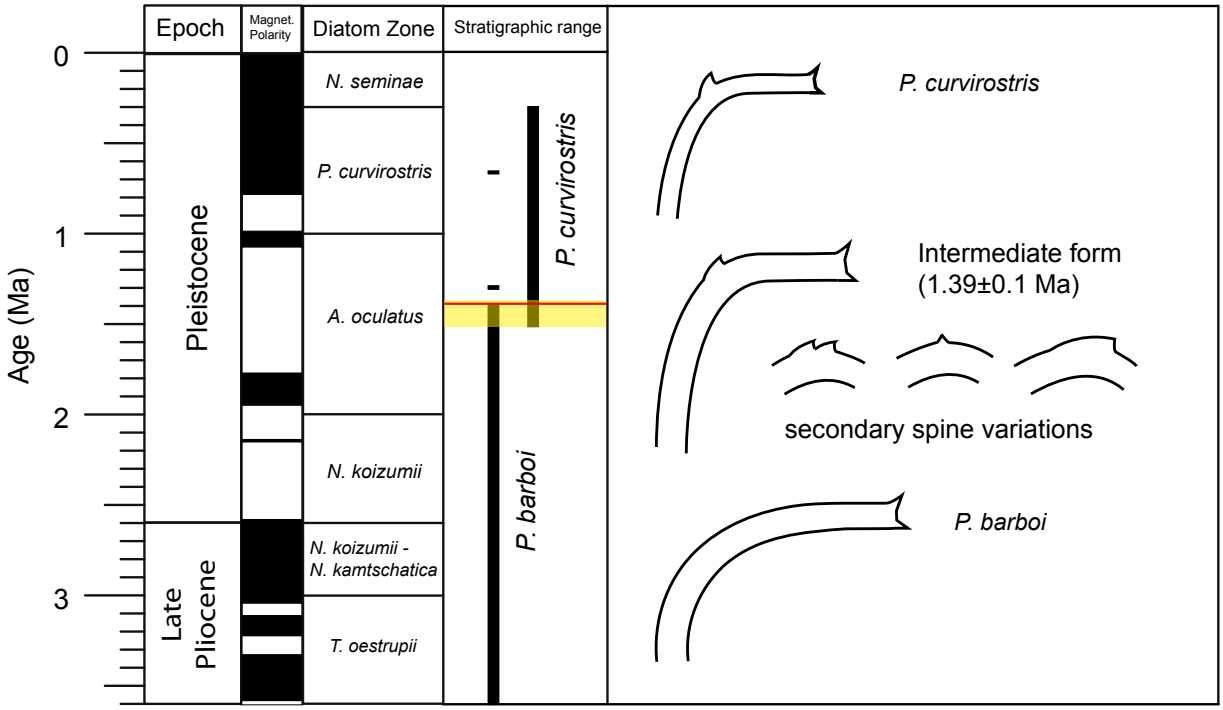

FIGURE 10. Stratigraphic range of *P. barboi* and *P. curvirostris* in Core U1340A (this study; Stroynowski *et al.*, 2015). Red horizontal line signals the appearance of the intermediate forms (Sample U1340A-24H-5; 1.39±0.1Ma) and the yellow bar indicates the interval where specimens with variations of the secondary spine occur. On the right, schematic morphology of *P. barboi*, *P. curvirostris*, and intermediate forms, illustrating the differences in length, width, curvature, the secondary spine and its variations. Diatom zonation of Koizumi *et al.* (2009). Magnetochronology from Cande and Kent (1995; CK 95).

The stratigraphic position of intermediate forms from Sample U1340A-24H-5 coincides with the interval expected for an evolutionary transition (*Actinocyclus oculatus* Zone; Fig. 10). According to this scenario, *P. barboi* would have developed a spine at the point of strongest curvature and diminished the length, width and curvature of the whole proboscis, ultimately giving rise to *P. curvirostris*. Specimens with an incipient secondary spine would represent the early stage in this evolutionary process. However, this speciation should have happened before 1.39Ma since *P. curvirostris* already appears at 1.52Ma in Site U1340. Likewise, the same species has been reported in older sediments of other regions of the North Pacific, the earliest FO being at 1.9Ma in Sites 192 and 183 of the Subarctic (Koizumi, 1973; Koizumi, 2010). It is possible that the intermediate forms were overlooked in other sites of the North Pacific due to rarity or because most studies are biostratigraphic in nature and cover numerous diatom taxa. Thus, it is necessary to check samples close to the *P. curvirostris* FO in other sites, particularly in Sites 192 and 183, to determine the stratigraphic range of the intermediate forms. Given that *P. barboi* co-occurs with *P. curvirostris* in the North Pacific this evolutionary process was cladogenetic.

Future research may determine whether these intermediate forms occur in the North Atlantic, and further corroborate the hypothesis for an evolutionary transition. It is interesting to notice that, the speciation of *P. curvirostris* may have been restricted to the Northern Hemisphere since *P. curvirostris* has never been reported in areas of the Southern Hemisphere, where only *P. barboi* is preserved (Jordan and Priddle, 1991).

Biotratigraphic analysis

Proboscia barboi displays an interesting stratigraphic distribution in Site U1340, as it disappears after the FCO of *Proboscia curvirostris* at 1.39Ma (Sample U1340A-24H-5), and only reappears at 0.67Ma, which is its LO (Sample U1340A-11H-CC). At Site U1341, *P. barboi* shows a regular occurrence with low abundance throughout the stratigraphic record until it disappears at 0.42-0.4Ma (Onodera *et al.*, 2016). The contrasting stratigraphic distributions of *P. barboi* at Sites U1341 and U1340 could be explained by environmental conditions such as the differential influence of sea ice in the eastern and western slopes of the Bowers Ridge.

In Site U1340, Takahashi *et al.*, 2011 (Expedition 323 Scientists, 2011) proposed that the LO of *P. barboi* occurs at 0.3Ma. One possible explanation for the lack of correspondence with the results reported herein is the

misidentification of *P. barboi*, as reported by Loseva (1990) in the Pleistocene of North Eastern Europe. She showed that the proboscis of *P. curvirostris* can split longitudinally, separating itself into two halves: one with the secondary spine and another without it, resembling the proboscis of *P. barboi*.

The FO of *P. curvirostris* was set at Sample U1340A-26H-5 (1.52Ma) based on the scarce specimens found therein. This datum falls in line with the FO's set in other sites of the North Pacific, which vary between 1.37 and 1.9Ma, depending on location (Barron and Gladenkov, 1995; Koizumi, 1973; Koizumi, 2010; Onodera *et al.*, 2016; Teraishi *et al.*, 2016; Yanagisawa and Akiba, 1998). Several reasons can account for this geographic diachrony, such as different oceanographic conditions. At Site U1341, in the western slope of Bowers Ridge the FO of *P. curvirostris* was observed at 1.37-1.42Ma, somewhat later than the one observed at Site U1340, located at the eastern slope (Fig. 1). At Site U1343, in the Bering slope, which is reached by the seasonal sea ice cover, the FO of *P. curvirostris* was observed at 1.7Ma (Teraishi *et al.*, 2016). This diachrony seems to form a trend by which the greater the sea ice influence of the location, the older the age of the FO of *P. curvirostris*. Other reasons for the diachrony of the *P. curvirostris*' FO could lie in different preservation conditions but also in the criteria used for its identification. Although further research is necessary to determine whether the intermediate forms occur in other sites of the Bering Sea and North Pacific, they have the potential to be used as biostratigraphic markers in the Bering Sea, since they are present consistently and abundantly at 1.39Ma in Site U1340 and may signal a shift in the oceanographic parameters of the Bering Sea.

CONCLUSION

This study provides a description of the morphology of *P. barboi* and *P. curvirostris* from Core U1340A (IODP Exploration 323) and a biostratigraphic and evolutionary analysis of these species. The major conclusions are:

i) *P. barboi* and *P. curvirostris* share many of their features such as the distal spines, spinulae, longitudinal slit and longitudinal striae. The two distal spines are perpendicular to one another (*i.e.* normal orientation) but in *P. barboi* they occasionally show a parallel orientation. Two types of longitudinal striae were identified: one restricted to the distal end and the other present along the proboscis length. The secondary spine is the diagnostic feature of *P. curvirostris*, and along with its smaller length and width, and stronger curvature, differentiates this species from *P. barboi*.

ii) Longitudinal ridges were observed in specimens of *P. curvirostris* from Sample U1340A-18H-3, along the length of the proboscis, sometimes interconnected by transversal ribs. They are strikingly similar to the ridges found in *Proboscia subarctica*, although not as linear and regular.

iii) *P. barboi* is the older species, extending back to the Middle Miocene. Its LCO occurs at 1.44Ma and is absent in almost every upper level until it reappears again on its LO at 0.67Ma.

iv) The FO of *P. curvirostris* was observed at 1.52Ma, and the FCO at 1.39Ma (Sample U1340A-24H-5). The LO was observed at 0.33Ma.

v) Abundant large specimens with secondary spine variations occur at 1.39Ma (Sample U1340A-24H-5, 203.54mbsf). They have here been considered intermediate forms between *P. barboi* and *P. curvirostris*, since they display a size and thickness characteristic of the former and a secondary spine, characteristic of the latter. The incipient type of secondary spine best represents the intermediate morphology.

vi) The intermediate forms are evidence for an evolutionary process where *P. barboi* developed a secondary spine and diminished the proportions of its proboscis, ultimately giving rise to *P. curvirostris*. The incipient secondary spine represents an early stage in the evolutionary process. However, this event must have happened before 1.39Ma, as *P. curvirostris* has been reported in the Subarctic at 1.9Ma. The co-occurrence of the two species in the North Pacific means the evolutionary event was cladogenetic.

vii) The abundant occurrence of intermediate forms in Core U1340A may constitute a bioevent for a short Pleistocene interval, around 1.39Ma, when intermediate forms thrived abundantly in the Bering Sea.

ACKNOWLEDGMENTS

The authors are grateful to Cremilde Monteiro (IPMA, Algés) and Cristina Ferraz (IPMA, Algés) for their laboratory technical assistance. The authors would also like to express their gratitude to the IODP Scientists and Crew of Expedition 323 to the Bering Sea. Lastly, we would like to thank Dr. Andrew Gladenkov and an anonymous reviewer for their review and helpful comments, and the editorial revision by Dr. Carles Martín Closas that greatly assisted in improving the manuscript.

This work was partially supported by CCMAR (PEstC/MAR/LA0015/2013) and Project UID/GEO/04035/2013 funded by FCT - Fundação para a Ciência e a Tecnologia, in Portugal.

REFERENCES

Abrantes, F., Gil, I., Lopes, C., Castro, M., 2005. Quantitative diatom analyses - A faster cleaning procedure. Deep-Sea Research Part I: Oceanographic Research Papers, 52(1), 189-198. https://doi.org/10.1016/j.dsr.2004.05.012

Akiba, F. 1986. Middle Miocene to Quaternary diatom biostratigraphy in the Nankai Trough and Japan Trench, and modified Lower Miocene through Quaternary diatom zones for middle-to-high latitudes of the North Pacific. Initial Reports of the Deep Sea Drilling Project, 87, 393-480. https://doi.org/10.2973/dsdp.proc.87.106.1986

Akiba, F., Yanagisawa, Y., 1986. Taxonomy, morphology and phylogeny of the Neogene diatom zonal marker species in the middle-to-high latitudes of the North Pacific. Initial Reports of the Deep Sea Drilling Project, 87, 483-554. https://doi.org/10.2973/dsdp.proc.87.107.1986

Barron, J., 1985. Late Eocene to Holocene diatom biostratigraphy of the equatorial Pacific Ocean, Deep Sea Drilling Project Leg 85. Initial Reports of the Deep Sea Drilling Project. US Government Printing Office, Washington, 85 (OCT), 413-456. https://doi.org/10.2973/dsdp.proc.85.108.1985

Barron, J.A., Gladenkov, A.Y., 1995. Early Miocene to Pleistocene diatom stratigraphy of Leg 145. Proceedings of the Ocean Drilling Program, Scientific Results, 145, 3-19. https://doi.org/10.2973/odp.proc.sr.145.101.1995

Cande, S.C., Kent, D.V., 1995. Revised calibration of geomagnetic polarity time scale for the Late Cretaceous and Cenozoic. Journal of Geophysical Research, 100, 6093-6095. https://doi.org/10.1029/94jb03098

Chappell, J., Omura, A., Esat, T., Mcculloch, M., Pandolfi, J., Ota, Y., Pillans, B., 1996. Reconciliation of late Quaternary sea levels derived from coral terraces Huon Peninsula with deep sea oxygen isotope records. Earth and Planetary Science Letters, 141, 227-236. https://doi.org/10.1016/0012-821x(96)00062-3

Expedition 323 Scientists, 2010. Bering Sea paleoceanography: Pliocene–Pleistocene paleoceanography and climate history of the Bering Sea. IODP Preliminary Report, 323, https://doi.org/10.1002/2015pa002866

Expedition 323 Scientists, 2011. Site U1340. In: Takahashi, K., Ravelo, A.C., Zarikian, C.A., the Expedition 323 Scientists, 2011. Proceedings IODP 323. Tokyo, Integrated Ocean Drilling Program Management International, 1-81. https://doi.org/10.2204/iodp.sd.11.01.2011

Hajós, M., 1976. Upper Eocene and lower Oligocene Diatomaceae, Archaeomonadaceae, and Silicoflagellatae in Southwestern Pacific Sediments, DSDP Leg 29. Initial Reports of the Deep Sea Drilling Project, 35, 817-883. https://doi.org/10.2973/dsdp.proc.35.29chap1.1976

Hargraves, P.E., 1986. The relationship of some fossil diatom genera to resting spores. Proceedings of the Eighth International Diatom Symposium. O. Koeltz, Koenigstein, 67-80.

Hasle, G.R., Syvertsen, E.E., Steidinger, K.A., Tangen, K., Tomas, C.R., 1996. Identifying marine diatoms and dinoflagellates. Academic Press, 598pp. https://doi.org/10.1016/b978-012693015-3/50006-1

Jordan, R.W., Ligowski, L., Nöthig, E.M., Priddle, J., 1991. The diatom genus *Proboscia* in Antarctic waters. Diatom Research, 6.1, 63-78. https://doi.org/10.1080/0269249x.1991.9705148

Jordan, R.W., Priddle, J., 1991. Fossil members of the diatom genus *Proboscia*. Diatom Research, 6(1), 55-61. https://doi.org/10.1080/0269249X.1991.9705147

Jordan, R.W., Saito, M., 1999. The genus *Proboscia* from the *Thalassiosira yabei* zone (middle-late Miocene) sediments of Hokkaido, Japan. In: Mayama, S., Idei, M., Koizumi, I. (eds.). Proceedings of the Fourteenth International Diatom Symposium. Tokyo (Japan), September 2-8, 1996. Koeltz Scientific Books, Koenigstein, 565-580

Jordan, R.W., Ito, R., 2002. Observations on *Proboscia* species from late Cretaceous sediments, and their possible evolution from Kreagra. In: John, J. (ed.). Proceedings of the 15th International Diatom Symposium. Perth (Australia), 28 September -2 October, 1998, A.R.G. Gantner Verlag K.G., 313-330.

Jordan, R.W., Ligowski, I.R., 2004. New observations on *Proboscia* auxospores and validation of the family Probosciaceae fam. nov. Vie et milieu, 54(2-3), 91-103.

Jouse, A.P., 1971. Diatoms in Pleistocene sediments from the northern Pacific Ocean. In: Funnell, B., Riedel, R. (eds.). The micropaleontology of oceans. Cambridge University Press, 407-421.

Katsuki, K., Takahashi, K., 2005. Diatoms as paleoenvironmental proxies for seasonal productivity, sea-ice and surface circulation in the Bering Sea during the late Quaternary. Deep-Sea Research Part II: Topical Studies in Oceanography, 52(16-18), 2110-2130. https://doi.org/10.1016/j.dsr2.2005.07.001

Koç, N., Scherer, R.P., 1996. Neogene diatom biostratigraphy of the Iceland Sea Site 907. In: Thiede, J., Mclntyhre, A.M., Firth, J.V., Johnson, G.L., Ruddiman, W.F. (eds.). Proceedings of the Ocean Drilling Program, Scientific Results. Ocean Drilling Program, Texas A&M University, College Station, 151, 61-74. https://doi.org/10.2973/odp.proc.sr.151.108.1996

Koç, N., Labeyrie, L., Manthé, S., Flower, B.P., Hodell, D.A., Aksu, A., 2001. The last occurrence of *Proboscia curvirostris* in the North Atlantic marine isotope stages 9-8. Marine Micropaleontology, 41(1), 9-23. https://doi.org/10.1016/S0377-8398(00)00054-2

Koizumi, I., 1973. The late Cenozoic diatoms of Sites 183–193, Leg 19 Deep Sea Drilling Project. In: Creager, J.S., Scholl, D.W., P.R. (eds.). Initial Reports of the Deep Sea Drilling Project, 19(30), 805-855. https://doi.org/10.2973/dsdp.proc.19.130.1973

Koizumi, I., Tanimura, Y., 1985. Neogene latitude biostratigraphy of the middle latitude western North Pacific, Deep Sea Drilling Project Leg 86. Initial Reports of the Deep Sea Drilling Project, 86, 269-300. https://doi.org/10.2973/dsdp.proc.86.109.1985

Koizumi, I., Sato, M., Matoba, Y., 2009. Neogene diatoms from the Oga Peninsula, North-East Japan and ODP drilling cores in the Japan Sea. Palaeogeography, Palaeoclimatology,

Palaeoecology, 272, 85-98. https://doi.org/10.1016/j.palaeo.2008.11.007

Koizumi, I., 2010. Revised diatom biostratigraphy of DSDP Leg 19 drill cores and dredged samples from the subarctic Pacific and Bering Sea. JAMSTEC Report of Research and Development, 10, 1-23. https://doi.org/10.5918/jamstecr.10.1

Loseva, E., 1990. Are Both *Rhizosolenia curvirostris* Jouse and *R. barboi* Brun found in Pleistocene Sediments of Northeastern Europe? 11th International Diatom Symposium, 55-61.

Mann, D.G., 1999. The species concept in diatoms. Phycologia, 38(6), 437-495. https://doi.org/10.2216/i0031-8884-38-6-437.1

Onodera, J., Takahashi, K., Nagatomo, R., 2016. Diatoms, silicoflagellates, and ebridians at Site U1341 on the western slope of Bowers Ridge, IODP Expedition 323. Deep-Sea Research Part II: Topical Studies in Oceanography, 125, 8-17. https://doi.org/10.1016/j.dsr2.2013.03.025

Sancetta, C., Silvestri, S., 1986. Pliocene-Pleistocene evolution of the North Pacific Ocean-Atmosphere system, interpreted from fossil diatoms. Paleoceanography, 1(2), 163-180. https://doi.org/10.1029/PA001i002p00163

Schrader, H.J., 1973. Cenozoic diatoms from the North-East Pacific, Leg 18. Initial Reports of the Deep Sea Drilling Project, 18, 673-797. https://doi.org/10.2973/dsdp.proc.18.117.1973

Stabeno, P.J., Schumacher, J.D., Ohtani, K., 1999. The physical oceanography of the Bering Sea. In: Loughlin, T.R., Ohtani, K. (eds.). Dynamics of the Bering Sea: A Summary of Physical, Chemical, and Biological Characteristics, and a Synopsis of Research on the Bering Sea, North Pacific Marine Science Organization (PICES), University of Alaska Sea Grant, AK-SG-99-03, Fairbanks, Alaska, USA, 1-28

Stroynowski, Z., Ravelo, A.C., Andreasen, D., 2015. A Pliocene to recent history of the Bering Sea at Site U1340A, IODP Expedition 323. Paleoceanography, 30(12), 1641-1656. https://doi.org/10.1002/2015pa002866

Stroynowski, Z., Abrantes, F., Bruno, E., 2017. The response of the Bering Sea Gateway during the Mid-Pleistocene Transition. Palaeogeography, Palaeoclimatology, Palaeoecology, 485, 974-985. https://doi.org/10.1016/j.palaeo.2017.08.023

Takahashi, K., Jordan, R., Priddle, J., 1994. The diatom genus - in Subarctic Waters. Diatom Research, 9(2), 411-428. https://doi.org/10.1080/0269249X.1994.9705317

Takahashi, K., 2005. The Bering Sea and paleoceanography. Deep-Sea Research Part II: Topical Studies in Oceanography, 52(16-18), 2080-2091. https://doi.org/10.1016/j.dsr2.2005.08.003

Takahashi, K., Ravelo, A.C., Zarikian, C.A., 2011. IODP Expedition 323 - Pliocene and Pleistocene paleoceanographic changes in the Bering Sea. Scientific Drilling, 11, 4-13. https://doi.org/10.2204/iodp.sd.11.01.2011

Teraishi, A., Suto, I., Onodera, J., Takahashi, K., 2016. Diatom, silicoflagellate and ebridian biostratigraphy and paleoceanography in IODP 323 Hole U1343E at the Bering slope site. Deep-Sea Research Part II: Topical Studies in Oceanography, 125, 18-28. https://doi.org/10.1016/j.dsr2.2013.03.026

Tréguer, P.J., De La Rocha, C.L., 2013. The world ocean silica cycle. Annual Review of Marine Science, 5(1), 477-501. https://doi.org/10.1146/annurev-marine-121211-172346

Tsukazaki, C., Ishii, K.I., Saito, R., Matsuno, K., Yamaguchi, A., Imai, I., 2013. Distribution of viable diatom resting stage cells in bottom sediments of the eastern Bering Sea shelf. Deep-Sea Research Part II: Topical Studies in Oceanography, 94, 22-30. https://doi.org/10.1016/j.dsr2.2013.03.020

Yanagisawa, Y., Akiba, F., 1998. Refined Neogene diatom biostratigraphy for the North-West Pacific around Japan, with an introduction of code numbers for selected diatom biohorizons. Journal of the Geological Society of Japan, 24(6), 395-414. https://doi.org/10.5575/geosoc.104.395

Manuscript received September 2018;
revision accepted July 2019;
published Online October 2019.